Korean J. Chem. Eng., 37(7), 1218-1225 (2020)
DOI: 10.1007/s11814-020-0544-z

pISSN: 0256-1115
eISSN: 1975-7220

Nitrogen and sulfur dual-doped porous carbon derived from coffee waste and cysteine for electrochemical energy storage

Jumi Hong[*,], Harim Kim[***], Ji Eun Lee[*], You Na Ko[*], Ki Tae Park[*], Young Eun Kim[*], Min Hye Youn[*], Soon Kwan Jeong[*], Jinwon Park[**,†,‡], and Wonhee Lee[*,†,‡]**

*Climate Change Research Division, Korea Institute of Energy Research (KIER), 152 Gajeong-ro, Yuseong-gu, Daejeon 34129, Korea
**School of Chemical and Biomolecular Engineering, Yonsei University, 50 Yonsei-ro, Seodaemun-gu, Seoul 03722, Korea
***Department of Chemistry, College of Natural Sciences, Yeungnam University, Gyeongsan, Gyeongbuk 38541, Korea
(*Received 10 September 2019 • Revised 22 February 2020 • Accepted 16 March 2020*)

Abstract−N/S dual-doped carbon materials were synthesized from coffee waste and cysteine for use as porous carbon electrode materials for electric double layer capacitors. The capacitance of the carbon materials was calculated from the experimental results of cyclic voltammetry and galvanostatic charge-discharge tests. The N/S-doped carbon materials obtained from heat-treatment with cysteine exhibited a higher discharge capacitance, 71.3 F/g, than that of the carbon without the cysteine treatment, 43.8 F/g, at 1 A/g. This is because the N/S dual-doped carbons possess a higher wettability than that of the other carbon material, even though the N/S doping with cysteine destroys the porous carbon structure, which reduces the BET surface area of the carbon samples. Elemental analysis was performed to determine the portions of nitrogen and sulfur elements doped into the carbon. From the XPS results, various states of nitrogen and sulfur elements were identified, and SEM/TEM images were obtained to observe their morphologies and porous structures.

Keywords: Electric Double Layer Capacitor, Heteroatom Doping, Carbon, Coffee Waste, Cysteine

INTRODUCTION

Supercapacitors are energy storage devices that have received much interest due to their intrinsic advantages compared with other electrochemical systems. They are characterized by having a higher power density, higher charging/discharging efficiency, and longer life cycle time than most batteries [1-3]. There are various types of capacitors, such as dielectric, double-layer, and oxide/polymer redox films, and their mechanisms of energy storage are non-Faradaic electrostatic or Faradaic charge transfer [1,4]. The electrostatic energy storage of the supercapacitor is achieved by the formation of an electric double layer (EDL), which is an array of electrolyte charge accumulation on the electrode, and thus, the electric double layer capacitors (EDLCs) are the representative type of supercapacitors adapting that mechanism [1,4]. The high specific capacitance of the EDLCs originates from the EDL formed in the porous electrodes with a large surface area [1,2,5]. Various carbon materials, such as activated carbons [6-8] and carbon aerogels [7,9,10], are widely used in EDLC electrodes due to their high conductivity and highly porous structure [1,3]. Faradaic charge transfer can also be another electrical energy storage principle, and the supercapacitors adapting this mechanism are called pseudocapacitors [1,4]. Unlike EDLCs, various metal oxides [11-13] and conducting polymers [14,15] are used for the electrode materials for pseudocapacitors.

Recently, heteroatom-doped carbons have been investigated as another potential candidate of electrode materials for various electrochemical applications [16-20]. The change in the charge density of a carbon material is induced by the doping of heteroatoms, such as nitrogen (N), boron (B), sulfur (S), and phosphorus (P), into the carbon structure [16]. Additionally, some researchers have tried to obtain carbon materials from the pyrolysis of a biomass to utilize them as electrode materials [6,21-26]. Among them, coffee waste is the most discarded biomass, and it was reported that the carbon materials from coffee waste can be used for electrochemical applications [21-23,25]. Coffee waste contains nitrogen because it consists of polysaccharides, proteins, non-protein nitrogenous compounds, lipids, minerals, and phenolic compounds [27]. The existence of nitrogen in coffee waste induces self-nitrogen-doping into the carbon structure after pyrolysis [21-23,25]. Recently, many studies have investigated the doping of multiple elements into the carbon structure to improve the electrochemical performance of the carbon materials [16,18,28].

In this study, N/S dual-doped carbon materials derived from coffee waste and cysteine were created and utilized as electrode materials for an EDLC application. Because cysteine contains both nitrogen and sulfur atoms in its molecular structure, it can provide these elements into carbon for doping [29,30]. Cyclic voltammograms were obtained to calculate the specific capacitance of the resultant carbon materials. Galvanostatic charge-discharge tests were also performed to cross-check their capacitance. The BET surface

†To whom correspondence should be addressed.
E-mail: whlee@kier.re.kr, jwpark@yonsei.ac.kr
‡Jinwon Park and Wonhee Lee contributed equally to this work and share corresponding authorship.
Copyright by The Korean Institute of Chemical Engineers.

area of the N/S dual-doped carbon materials was measured. Scanning electron microscopy (SEM) and transmission electron microscopy (TEM) images were acquired to observe their surface morphology. The X-ray diffraction (XRD) patterns were measured, and X-ray photoelectron spectroscopy (XPS) data were also obtained to determine the types of bonds for the nitrogen and sulfur elements doped into the carbon. A cycle stability test was performed as well using the N/S-doped carbon material which showed the highest performance.

EXPERIMENTAL

1. Materials

Coffee waste was obtained from commercially available coffee beans after brewing. Zinc chloride ($ZnCl_2$, 98%), polytetrafluoroethylene (PTFE) preparation (60 wt% dispersion in H_2O), and hydrogen chloric acid (HCl, 37 wt% in water) were supplied by Sigma-Aldrich. Potassium hydroxide (KOH, 95%) was obtained from Unid (Korea), and ethanol (EtOH, 99.9%) was acquired from Duksan Reagents. Argon (Ar, 99.999%) was supplied by Special Gas (Korea). Deionized water (DI water) was acquired by a water purification system (Zeneer Power II, Human Corporation).

2. Synthesis of the Porous Carbon Doped by Nitrogen and Sulfur

First, coffee waste was dried in a vacuum oven at 80 °C over three days, and the dried coffee waste was ground with pestle in a mortar The coffee waste powder was heat-treated under 100 cm^3/min of an Ar flow in a horizontal tube furnace at 800 °C for 3 h (5 °C/min of heating rate). The resultant product was washed using EtOH, 5 M HCl solution (from 37 wt% of HCl solution by adding a stoichiometric amount of DI water) and DI water several times until the pH reached 7. After drying in a vacuum oven at 80 °C, the coffee waste product and $ZnCl_2$ were mixed with a weight ratio of 1 : 3 and ground. DI water was added to the coffee waste-$ZnCl_2$ mixture to dissolve the $ZnCl_2$ to be well dispersed into the coffee waste. After sonication and drying in the vacuum oven to remove the water, the coffee waste-$ZnCl_2$ mixture was ground. Then, the sample was activated by heat-treatment under 100 cm^3/min of an Ar flow at 800 °C for 3 h (5 °C/min of heating rate). Some of this sample was washed with EtOH, 5 M HCl solution and DI water. After drying, it was tested as an electrode material for EDLC (sample name: CW).

The rest of the sample was used for the N/S dual doping to carbon with cysteine. CW and cysteine were mixed with a weight ratio of 1 : 0.3 and 1 : 1. DI water was added to dissolve the cysteine completely, and the samples were sonicated for 20 min. After drying and grinding, they were heat-treated under 100 cm^3/min of an Ar flow at 800 °C for 3 h (5 °C/min of heating rate). Finally, the samples were washed with EtOH, 5 M HCl solution, and DI water, dried in the vacuum oven, and used for the other electrode materials for EDLC (sample names: CWCy30, CWCy100).

3. Electrochemical Analysis

Every electrochemical measurement involved using a three-electrode system and potentiostat/galvanostat/EIS system (SP-300, Biologic). The carbon samples (CW, CWCy30, and CWCy100; active materials) were mixed with PTFE (60% dispersed in water, a binder) in water (95 : 5 weight ratio). These carbon slurries were deposited on nickel foams (1 cm×1 cm; current collector), pressed and dried at 80 °C overnight to prepare working electrodes. 4 mg of the carbon active materials was loaded on the working electrodes (4 mg of a carbon active material/cm^2). A platinum wire was used as a counter electrode and Ag/AgCl as a reference electrode. Cyclic voltammetry and galvanostatic charge/discharge measurements were performed depending on the scan rate and current density in a 6 M KOH solution. The specific capacitance was calculated by the following equations:

$$C = \frac{I}{2m\left(\frac{dV}{dt}\right)} \quad \text{for cyclic voltammogram}$$

$$C = \frac{I\Delta t}{m\Delta V} \quad \text{for galvanostatic charge/discharge}$$

where C, I, dV/dt, ΔV, m, and Δt indicate the specific capacitance, current, scan rate, potential window excluding IR drop, mass of the active material, and discharging time, respectively. The cycle stability test was performed using CWCy30 at a current density of 1 A/g.

4. Characterization

The surface area of the coffee waste-derived carbon samples

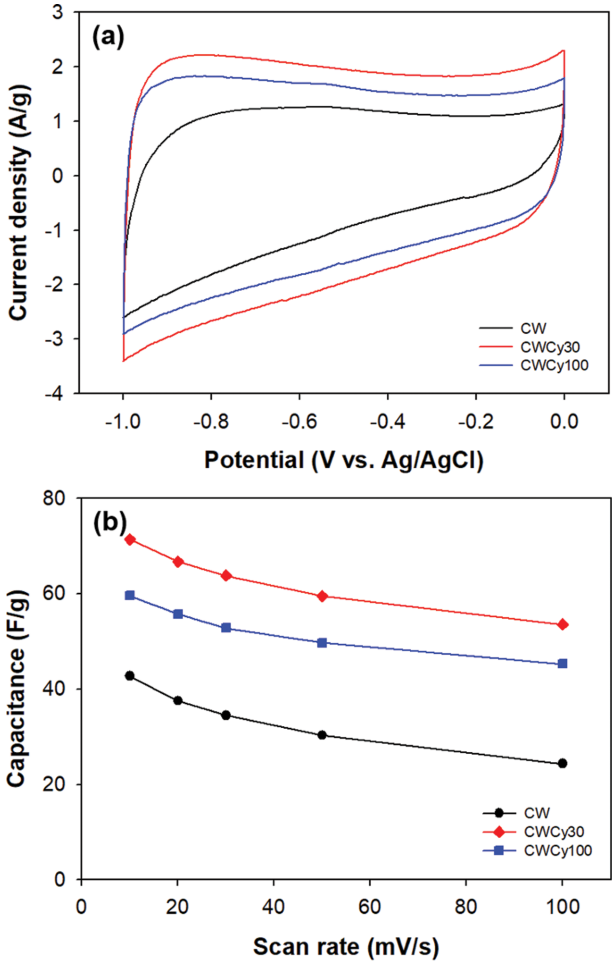


Fig. 1. (a) Cyclic voltammograms of the carbon samples derived from the coffee waste at 30 mV/sec and (b) specific capacitance calculated from the CV depending on the scan rate.

was measured using a BET & pore size analyzer (TriStar II 3020, Micromeritics) by the Brunauer-Emmett-Teller (BET) method from the N_2 adsorption-desorption isotherms at 77 K. The elemental compositions of the samples were determined by an elemental analyzer (FLASH 2000 series, Thermo Scientific). XPS data were obtained by a multipurpose X-ray photoelectron spectrometer (with UPS, Sigma Probe, Thermo VG Scientific). The XRD patterns of the carbon materials were measured by high resolution powder X-ray diffractometer (SmartLab, Rigaku) with a Cu Kα (λ=0.15418 nm) source. SEM images were obtained using a field emission SEM (SU8230, Hitachi) to observe the morphology of the carbon materials. TEM images were acquired using a field emission TEM at an operation voltage of 300 kV (Tecnai G2 F30 S-Twin, FEI company).

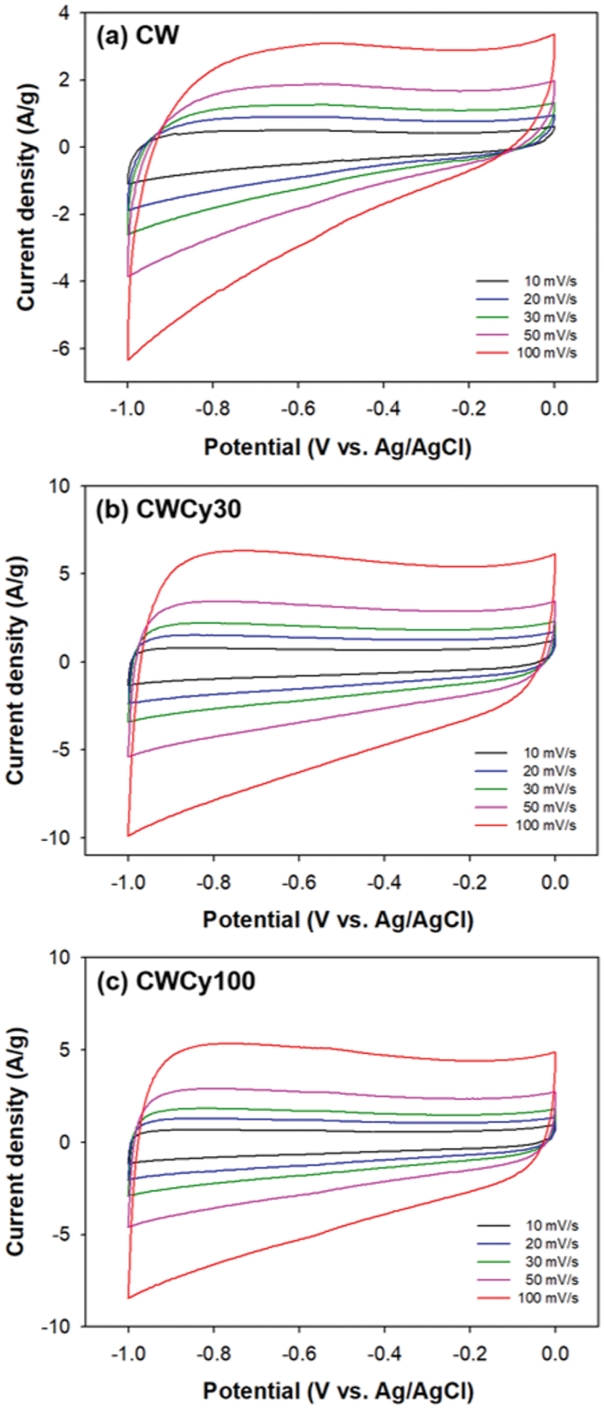


Fig. 2. (a) Cyclic voltammograms of (a) CW, (b) CWCy30, and (c) CWCy100 depending on the scan rate.

RESULTS AND DISCUSSION

Fig. 1(a) and (b) show the cyclic voltammograms of the carbon materials derived from the coffee waste at 30 mV/sec, and the specific capacitances of the materials depending on the scan rate calculated from the cyclic voltammograms, respectively. No Faradaic redox peaks are observed in these cyclic voltammograms, and thus, the capacitance mainly originates from the formation of the EDL rather than the Faradaic charge transfer. The specific capacitance of the carbon samples, CW, CWCy30 and CWCy100, was 42.7, 71.3, and 59.6 F/g at 10 mV/sec and 24.3, 53.5, and 45.3 F/g at 100 mV/sec. The capacitance decreased with the increase in the scan rate, which is the general trend of the specific capacitance variation as a function of the scan rate. All cyclic voltammograms of the three carbon samples at different scan rates are shown in Fig. 2. Fig. 3(a) and (b) show the galvanostatic charge-discharge curves of the same carbon materials at 1 A/g and the discharge capacitance as a func-

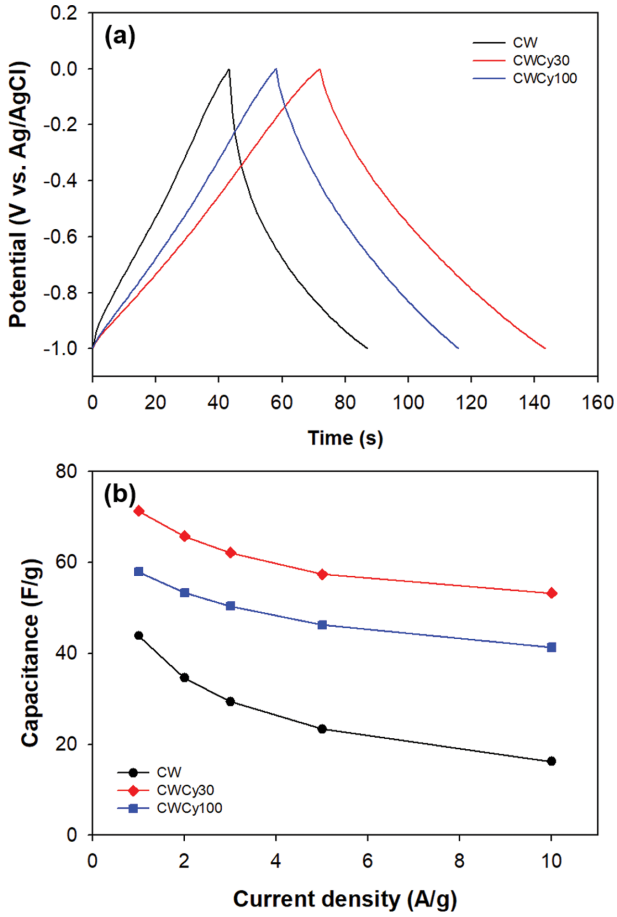


Fig. 3. (a) Galvanostatic charge/discharge profiles at a current density of 1 A/g and (b) discharge capacitance of the carbon samples derived from the coffee waste.

tion of the current density, respectively. The discharge capacitance of CW, CWCy30 and CWCy100 was 43.8, 71.3, and 57.9 F/g at 1 A/g and 16.2, 53.2, and 41.3 F/g at 10 A/g. The capacitance decreased with the increase in the current density, which is the general trend of the discharge capacitance depending on the current density. All galvanostatic charge-discharge curves of the three carbon samples at different scan rates are shown in Fig. 4. Regardless of the scan rate for the CV and the current density for galvanostatic charge-discharge tests, the capacitance of the carbon electrodes increased by the following order: CW<CWCy100<CWCy30.

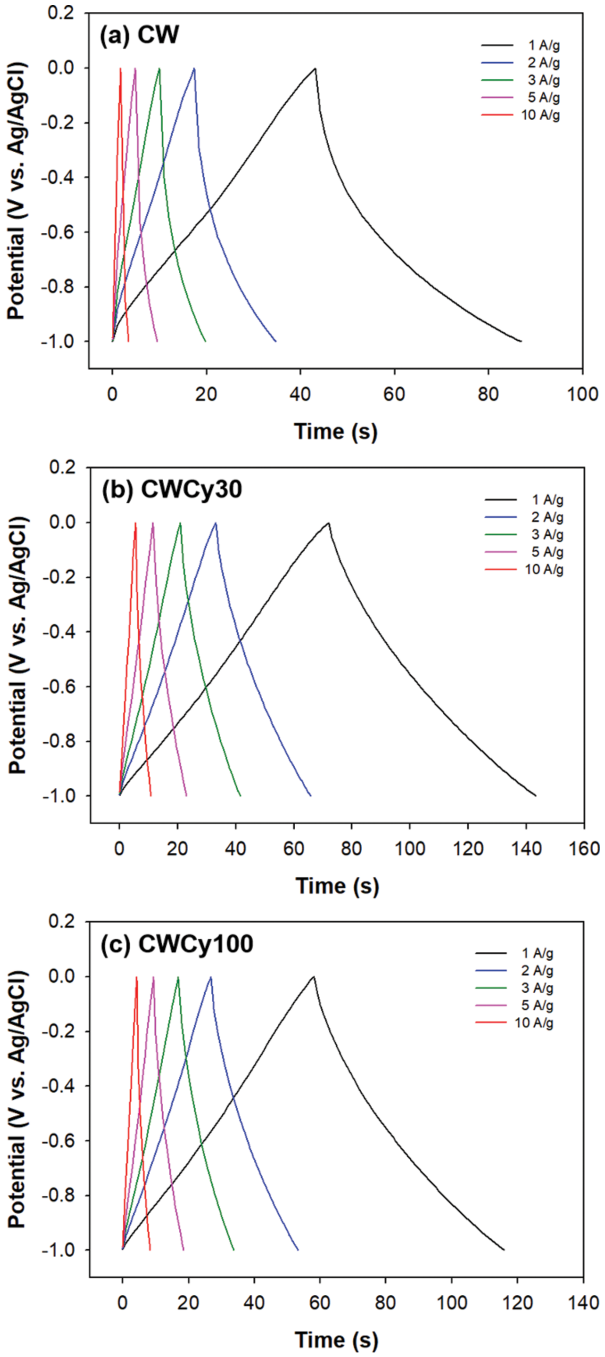


Fig. 4. Galvanostatic charge/discharge profiles of (a) CW, (b) CWCy30, and (c) CWCy100 depending on the current density.

After the activation with $ZnCl_2$ for all the samples, CW was not further heat-treated with cysteine, but the other samples were N/S dual-doped by the heat-treatment using cysteine with different ratios. Due to the different procedures for the heat-treatment, the BET surface areas of the carbon materials were measured, and elemental analysis was performed for the coffee waste-derived carbons because this data profoundly affects the specific capacitance of the carbon materials. Table 1 lists the BET surface areas of the CW, CWCy30 and CWCy100 which were 893, 743, and 630 m^2/g, respectively. The interesting point is that even though the N/S dual-doped carbon samples, CWCy30 and CWCy100, have a lower BET surface area, their capacitances are higher than that of CW. This implies that N/S dual doping to carbon can be an important treatment for the enhanced capacitance.

From the N_2 adsorption/desorption measurements, type IV isotherms were observed for all the carbon samples shown in Fig. 5. This implies that all the samples derived from the coffee waste possess some portion of mesopores. Thus, all the carbon samples exhibit a hierarchically porous structure. Table 1 also includes the surface areas of the micropores (<2 nm) and the summation of mesopore (2 nm≤mesopore≤50 nm) and macropore (>50 nm). CW has a microporous and meso and macroporous area of 416 and 477 m^2/g, respectively. CWCy30 and CWCy100 have a microporous and meso and macroporous area of 289 and 454 m^2/g and 236 and 394 m^2/g, respectively. Fig. 6. shows the incremental pore area of the carbon samples depending on the average pore diameter, respectively. It does not exhibit the surface area of average pore diameter smaller than 1.7 nm (mainly meso- and macropore regions shown). Even though the surface area distribution depending on the pore size is quite similar, regardless of the sample, more micro-

Table 1. Pore textural properties of the carbon samples derived from the coffee waste

Data	CW	CWCy30	CWCy100
S_{BET} (m^2/g)	893	743	630
S_{micro} (m^2/g, <2 nm)	416	289	236
$S_{meso+macro}$ (m^2/g, ≥2 nm)	477	454	394

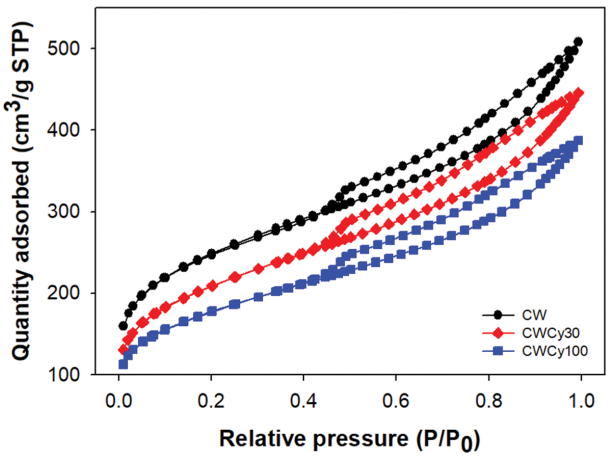


Fig. 5. N_2 adsorption-desorption isotherms of the carbon samples derived from the coffee waste.

porous area was reduced in the N/S-doped carbon derived from the heat treatment with more cysteine. This result implies that further heat-treatment using cysteine sacrificed the surface area of the carbon to dope the heteroatoms, nitrogen and sulfur, into the carbon structure. In addition, the utilization of more cysteine induced more carbon destruction. The post-treatment strategy, which is the modification of the carbon nanomaterials already created with various N sources, [31,32] generally might destroy the carbon lattice, influencing the morphology and pore size [33]. Furthermore, surface sulfurization is also known to reduce the surface area of carbon materials significantly and to distort the porous structure leading to micropore blockage [34]. The porous structure of the carbon samples in this study seemed to undergo distortion and destruction by the N/S dual-doping due to the reduction of the surface area, especially for the micropores.

Table 2 lists the results of the elemental analysis to confirm the portion of N and S doped into the carbon structures by the heat-treatment using cysteine. CW has 2.07 wt% of N and 0.14 wt% of S in its structure. Even though CW was not further heat-treated with cysteine, 2.07 wt% of N was self-doped into CW because the coffee waste contained the N element in itself [27]. In comparison with the CW, CWCy30 and CWCy100 contain 2.54 wt% of N for both samples, and 3.68 wt% and 3.31 wt% of S that were doped into their carbon structures. The increased portion of N and S originated from the heat-treatment with cysteine as an N/S source. Even though the surface area of CW is higher than the others, the specific capacitance of CW is much lower than that of CWCy30 and CWCy100. The higher capacitance of the N/S dual-doped carbons appears to originate from the enhancement of wettability arising from the existence of the N/S atoms in the carbon structure, which improves the contact of the ions in the electrolyte on the carbon electrodes [35]. By the way, the discharge capacitance of CWCy100 is lower than that of CWCy30. This is because the lower BET surface area of CWCy100, which arose from the heat-treatment using more cysteine severely destroying the carbon structure, despite the similar amount of N/S doped into the carbon materials derived from the coffee waste.

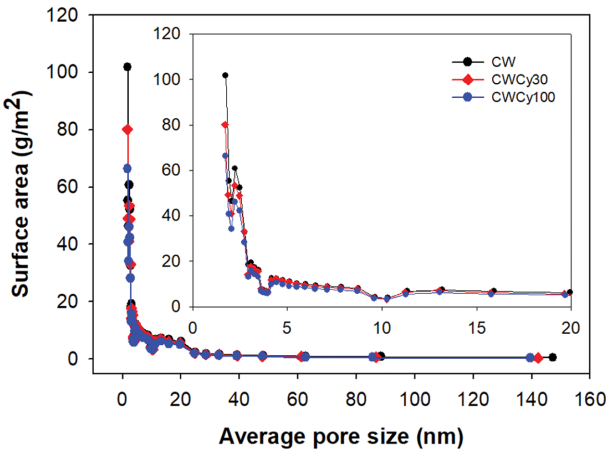


Fig. 6. Incremental pore area of the carbon samples depending on the average pore diameter.

Table 2. Elemental analysis results (wt%) of the carbon samples derived from the coffee waste

Elements	CW	CWCy30	CWCy100
C	89.00	86.38	85.45
H	1.23	0.73	0.88
N	2.07	2.54	2.54
S	0.14	3.68	3.31

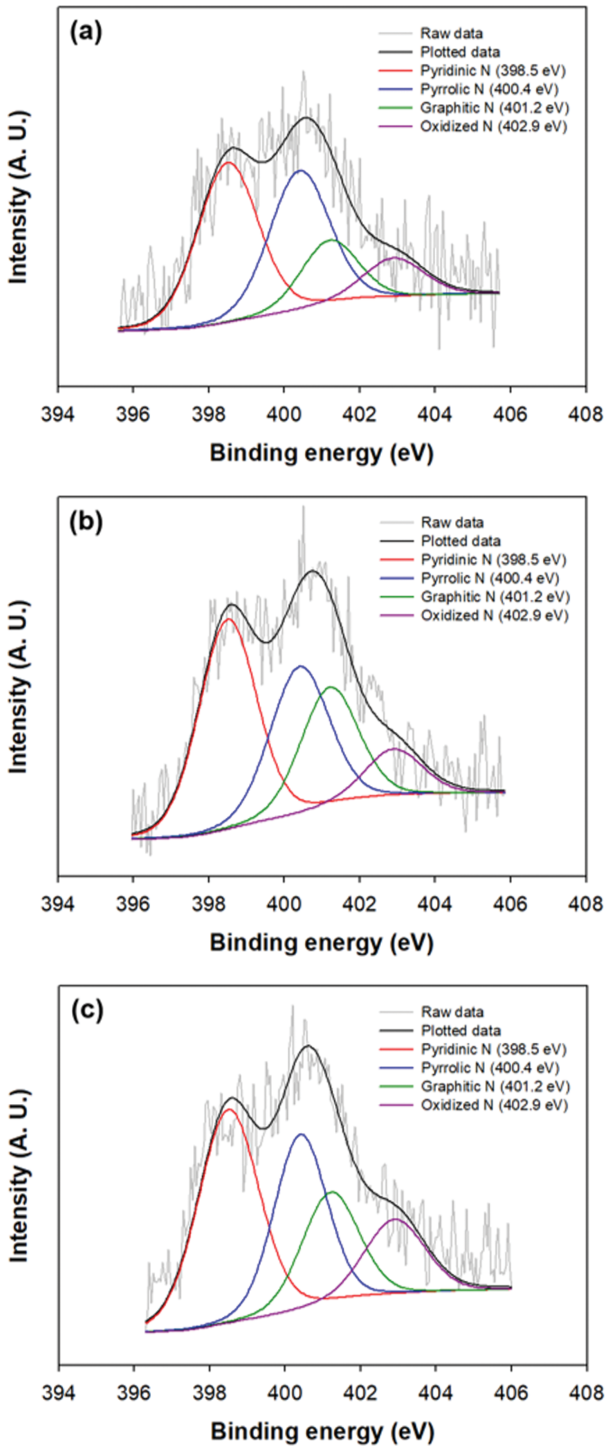


Fig. 7. XPS N1s spectra of (a) CW, (b) CWCy30, and (c) CWCy100.

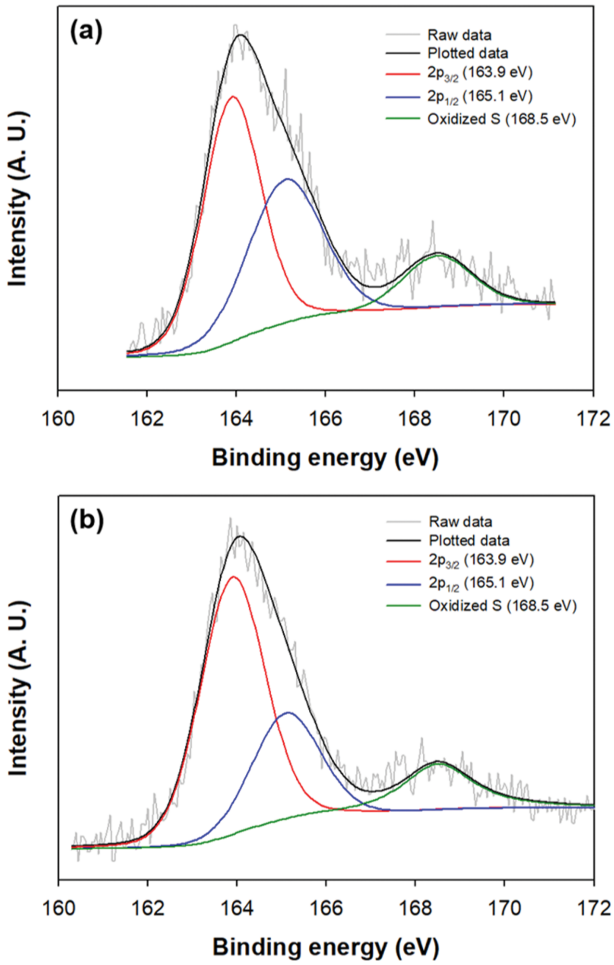


Fig. 8. XPS S2p spectra of (a) CWCy30 and (b) CWCy100.

Figs. 7 and 8 show the XPS N1 s and S2 p spectra of the carbon materials investigated using the coffee waste in this study. For all the carbon samples, the N1 s peaks at 398.5 eV, 400.4 eV, 401.2 eV, and 402.9 eV, which are pyridinic N, pyrrolic N, graphitic N, and oxidized N, respectively, [36,37] were observed. Additionally, the S2 p peaks at 163.9 eV, 165.1 eV, and 168.5 eV, which are $2p_{3/2}$, $2p_{1/2}$, and oxidized S [38], respectively, were observed. Due to these chemical bonds by the B/N doping, the wettability of the carbon materials heat-treated with cysteine seems to increase, which induces their specific capacitance.

Fig. 9 shows the XRD patterns of the three coffee waste-derived carbon materials studied in this paper. All the carbon samples exhibited two diffraction peaks at 2θ=24.9° and 43.5°. These are the XRD peaks of graphite carbon that are slightly shifted from those of previous studies, and their crystal planes are (002) and (101), respectively [39,40]. In addition, the position and broadness of the diffraction peaks were almost unchanged, and the peak height was slightly increased for CWCy30 and CWCy100, which are the cysteine-treated samples. This indicates that the heat-treatment using cysteine reduced the surface area of the carbon from the coffee waste, but their crystallinity was not significantly affected despite the structure distortion and destruction by the N/S doping.

The surface morphology of the carbon materials derived from

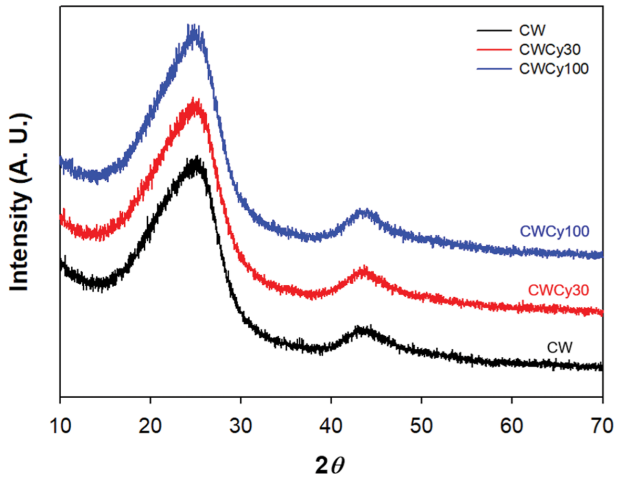


Fig. 9. XRD patterns of the carbon samples derived from the coffee waste.

coffee waste was investigated by SEM images shown in Fig. 10. Regardless of the N/S doping, all the carbon samples had a similar morphology. Above all, the SEM images show the interconnected spherical carbon particles that are around tens of nanometers in size. In addition, there are irregular voids that are tens or hundreds of nanometers in size between the interconnected carbon network. These voids and mesopores from the BET data would act as a passage for the electrolyte to penetrate inside the carbon materials.

Fig. 11 shows the TEM images of the heat-treated carbon materials with and without cysteine. TEM images of the carbon materials derived from the coffee waste revealed that all the samples had similar morphologies with mesoporous structures regardless of the different amount of the doping elements. This result indicates that there is no clear difference in the morphological feature of the carbon materials by the cysteine treatment effect and the morphology shown in the TEM images of the carbon samples originated from the $ZnCl_2$ activation.

A cycle stability test was performed at the galvanostatic charge-discharge mode at a current density of 1 A/g. CWCy30 was selected as an electrode material because it exhibited the highest capacitance among the carbon materials investigated in this study. After 1000 cycles of the stability test, CWCy30 maintained 91.3% of the initial discharge capacitance, shown in Fig. 12, which indicates a good repeated charge-discharge pattern.

CONCLUSIONS

The present work reports the synthesis of an N/S dual-doped carbon derived from coffee waste and cysteine for supercapacitor applications. The heteroatoms doped into the carbon originated from the cysteine that has both nitrogen and sulfur elements in its structure. The specific and discharge capacitances of the N/S-doped carbons were determined by cyclic voltammetry and galvanostatic charge-discharge tests, respectively. Among the carbon samples, CWCy30, which is the N/S-doped carbon synthesized by heat-treatment with the carbon from the coffee waste (CW) and cysteine with a weight ratio of 1 : 0.3, exhibited the highest discharge

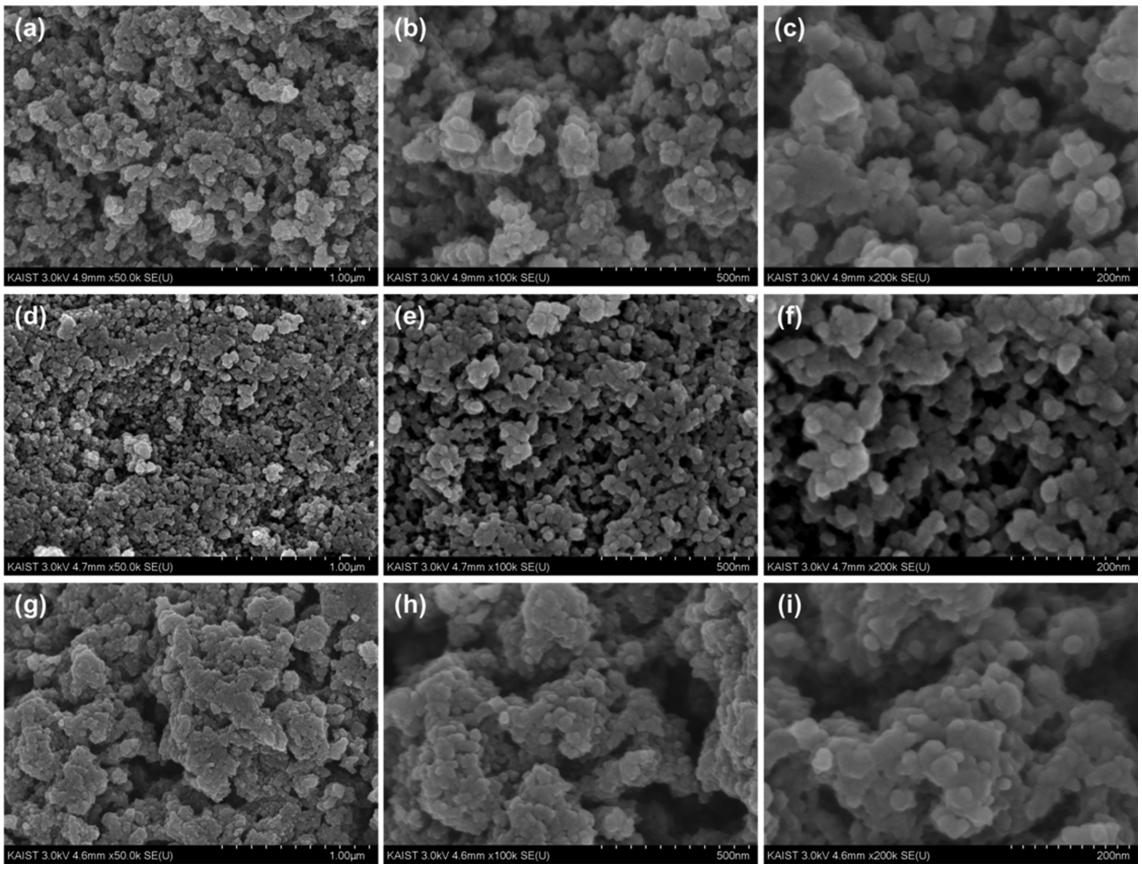


Fig. 10. SEM images of (a)-(c) CW, (d)-(f) CWCy30, and (g)-(i) CWCy100.

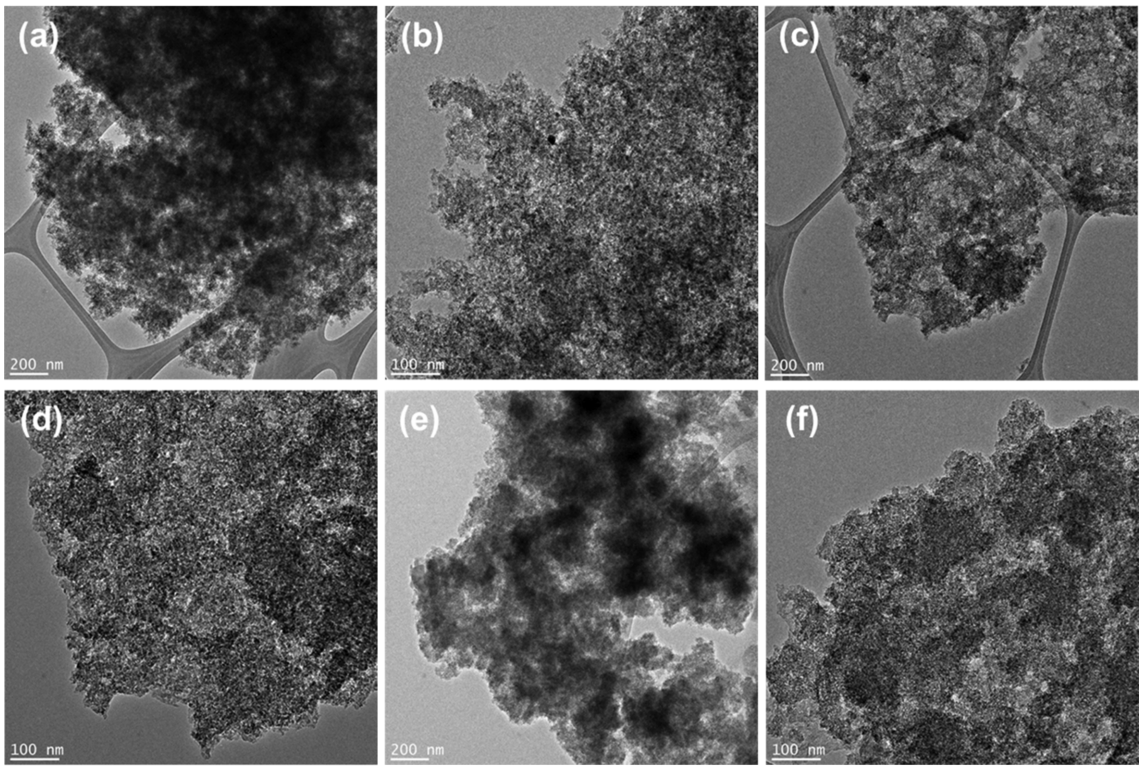


Fig. 11. TEM images (a)-(b) CW, (c)-(d) CWCy30, and (e)-(f) CWCy100.

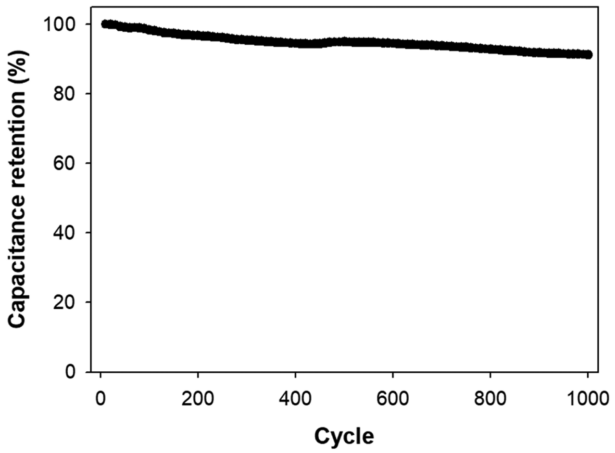


Fig. 12. The cycle stability test of CWCy30 at a current density of 1 A/g.

capacitance of 71.3 F/g. This originated from the improved wettability of the carbon material by the N/S dual-doping. Because the doping of the heteroatoms led to the destruction of the porous carbon structure, which induced the reduction of the BET surface area, the doping of too much of them reduced the capacitance. The XPS data showed the various states of the heteroatoms that enhance the wettability, and the SEM/TEM images also showed their morphologies and porous structures.

ACKNOWLEDGEMENT

This work was supported by the Korea Institute of Energy Technology Evaluation and Planning (KETEP) and the Ministry of Trade, Industry & Energy (MOTIE) of the Republic of Korea (No. 20182010202100).

REFERENCES

1. A. G. Pandolfo and A. F. Hollenkamp, *J. Power Sources*, **157**, 11 (2006).
2. M. D. Stoller and R. S. Ruoff, *J. Energy Environ. Sci.*, **3**, 1294 (2010).
3. L. Hao, X. Li and L. Zhi, *Adv. Mater.*, **25**, 3899 (2013).
4. B. E. Conway, *Electrochemical supercapacitors: Scientific fundamentals and technological applications*, Plenum Press, New York (1999).
5. P. Simon and Y. Gogotsi, *Nat. Mater.*, **7**, 845 (2008).
6. Y.-J. Kim, B.-J. Lee, H. Suezaki, T. Chino, Y. Abe, T. Yanagiura, K. C. Park and M. Endo, *Carbon*, **44**, 1592 (2006).
7. W. Lee, M. Kwon, S. Park, D. Lim, J.-H. Cha and H. Lee, *Chem.-Asian J.*, **8**, 1569 (2013).
8. K. S. Lee, M. Park, S. Choi and J.-D. Kim, *Colloids Surf. A: Physicochem. Eng. Aspects*, **529**, 107 (2017).
9. S. H. Kwon, E. Lee, B.-S. Kim, S.-G. Kim, B.-J. Lee, M.-S. Kim and J. C. Jung, *Korean J. Chem. Eng.*, **32**, 248 (2015).
10. I. Yang, D. Kwon, M.-S. Kim and J. C. Jung, *Carbon*, **132**, 503 (2018).
11. N. M. Shinde, A. D. Jagadale, V. S. Kumbhar, T. R. Rana, J. Kim and C. D. Lokhande, *Korean J. Chem. Eng.*, **32**, 974 (2015).
12. N. Venugopal and W.-S. Kim, *Korean J. Chem. Eng.*, **32**, 1918 (2015).
13. W.-J. Lee, S. Jeong, H. Lee, B.-J. Kim, K.-H. An, Y.-K. Park and S.-C. Jung, *Korean J. Chem. Eng.*, **34**, 2993 (2017).
14. J. Banerjee, K. Dutta, M. A. Kader and S. K. Nayak, *Polym. Adv. Technol.*, **30**, 1902 (2019).
15. Y. Tian, C. Yang, X. Song, J. Liu, L. Zhao, P. Zhang and L. Gao, *Chem. Eng. J.*, **374**, 59 (2019).
16. J. P. Paraknowitsch and A. Thomas, *J. Energy Environ. Sci.*, **6**, 2839 (2013).
17. Y. Kim, W. Lee, G. M. Kim and J. W. Lee, *RSC Adv.*, **6**, 54889 (2016).
18. W. Lee, G. M. Kim, S. Baik and J. W. Lee, *Electrochim. Acta*, **210**, 743 (2016).
19. A. Byeon, W. Lee, G. M. Kim and J. W. Lee, *J. CO_2 Util.*, **16**, 420 (2016).
20. Z. Yang, L. Xie, Y. Chen, T. Xue, B. Ma, K. Zhang, J. Zhao and J. Wei, *Appl. Surf. Sci.*, **493**, 1205 (2019).
21. Y. S. Yun, M. H. Park, S. J. Hong, M. E. Lee, Y. W. Park and H.-J. Jin, *ACS Appl. Mater. Interfaces*, **7**, 3684 (2015).
22. S. M. Unni, L. George, S. N. Bhange, R. N. Devi and S. Kurungot, *RSC Adv.*, **6**, 82103 (2016).
23. D. Y. Chung, Y. J. Son, J. M. Yoo, J. S. Kang, C.-Y. Ahn, S. Park, Y.-E. Sung, *ACS Appl. Mater. Interfaces*, **9**, 41303 (2017).
24. L. Jiang, L. Sheng and Z. Fan, *Sci. China Mater.*, **61**, 133 (2018).
25. A. Srinu, S. G. Peera, V. Parthiban, B. Bhuvaneshwari and A. K. Sahu, *Chem Select*, **3**, 690 (2018).
26. I. I. Misnon, N. K. M. Zain and R. Jose, *Waste Biomass Valoriz.*, **10**, 1731 (2019).
27. R. Campos-Vega, G. Loarca-Piña, H. A. Vergara-Castañeda, B. D. Oomah, *Trends Food Sci. Technol.*, **45**, 24 (2015).
28. J. Zhang, Z. Xia and L. Dai, *Sci. Adv.*, **1**, e1500564 (2015).
29. S. Niu, W. Lv, G. Zhou, Y. He, B. Li, Q.-H. Yang and F. Kang, *Chem. Commun.*, **51**, 17720 (2015).
30. H. Zhang, Y. Niu and W. Hu, *J. Colloid Interface Sci.*, **505**, 32 (2017).
31. Z.-S. Wu, W. Ren, L. Xu, F. Li and H.-M. Cheng, *ACS Nano*, **5**, 5463 (2011).
32. J. Liu, C. K. Poh, D. Zhan, L. Lai, S. H. Lim, L. Wang, X. Liu, N. G. Sahoo, C. Li, Z. Shen and J. Lin, *Nano Energy*, **2**, 377 (2013).
33. J. Wu, Z. Pan, Y. Zhang, B. Wang and H. Peng, *J. Mater. Chem. A*, **6**, 12932 (2018).
34. W. Kiciński, M. Szala and M. Bystrzejewski, *Carbon*, **68**, 1 (2014).
35. J. Yan, Q. Wang, T. Wei and Z. Fan, *Adv. Energy Mater.*, **4**, 1300816 (2014).
36. T. Wang, P. Zhang, Y. Sun, B. Liu, Y. Liu, Z.-A. Qiao, Q. Huo and S. Dai, *Chem. Mater.*, **29**, 4044 (2017).
37. T. Wang, Y. Sun, L. Zhang, K. Li, Y. Yi, S. Song, M. Li, Z.-A. Qiao and S. Dai, *Adv. Mater.*, **31**, 1807876 (2019).
38. B. Quan, S.-H. Yu, D. Y. Chung, A. Jin, J. H. Park, Y.-E. Sung and Y. Piao, *Sci. Rep.*, **4**, 5639 (2014).
39. C. Kim, J.-W. Lee, J.-H. Kim and K.-S. Yang, *Korean J. Chem. Eng.*, **23**, 592 (2006).
40. D. Yuan, J. Chen, J. Zeng and S. Tan, *Electrochem. Commun.*, **10**, 1067 (2008).